nature biomedical engineering

ARTICLES

https://doi.org/10.1038/s41551-019-0482-4

Identification and local delivery of vasodilators for the reduction of ureteral contractions

Christopher X. Lee[1,2], Jaime H. Cheah[2], Christian K. Soule[2], Huiming Ding[3], Charles A. Whittaker[3], Kyle Karhohs[4], Aurora A. Burds[2], Kriti S. Subramanyam[1,2], Anne E. Carpenter[4], Brian H. Eisner[5] and Michael J. Cima[1,2,6*]

Kidney stones and ureteral stents can cause ureteral colic and pain. By decreasing contractions in the ureter, clinically prescribed oral vasodilators may improve spontaneous stone passage rates and reduce the pain caused by ureteral stenting. We hypothesized that ureteral relaxation can be improved via the local administration of vasodilators and other smooth muscle relaxants. Here, by examining 18 candidate small molecules in an automated screening assay to determine the extent of ureteral relaxation, we show that the calcium channel blocker nifedipine and the Rho-kinase inhibitor ROCKi significantly relax human ureteral smooth muscle cells. We also show, by using ex vivo porcine ureter segments and sedated pigs that, with respect to the administration of a placebo, the local delivery of a clinically deployable formulation of the two drugs reduced ureteral contraction amplitude and frequency by 90% and 50%, respectively. Finally, we show that standard oral vasodilator therapy reduced contraction amplitude by only 50% and had a minimal effect on contraction frequency. Locally delivered ureteral relaxants therefore may improve ureter-related conditions.

The relaxation of the human ureter is beneficial for a wide variety of urological conditions. Examples include improving spontaneous expulsion rates and shortening the time to expulsion of ureteral stones[1], alleviating ureteral stent symptoms[2] and enabling safer passage of instruments through the ureter during endoscopic kidney stone surgery[3,4]. The lifetime prevalence of kidney stones alone is roughly 10%, and annual health incidence and healthcare costs in the United States exceed 2 million cases and US$5 billion annually[5–7].

The relaxation of the ureter is useful in several aspects of urology, including ureteroscopy procedures and treatment of patients with stent discomfort and ureteral stones[8–10]. Pharmacological inhibition of ureteral contractions allows ureteroscopies to be performed more safely, with decreased force required to insert sheaths into the ureteral lumen[3]. Pharmacological inhibition of ureteral contractions also has the potential both to shorten the time to ureteral stone passage and to increase the rate of spontaneous passage[11]. These effects significantly reduce pain and other symptoms, as well as the need for surgical intervention[8,12]. Irritation and stretch stimulation result in increased uncoordinated peristalsis, which increases pain and is believed to hinder stone passage[13].

The only method currently used to induce ureteral relaxation in patients with ureteral stent discomfort, ureteral stones, or for patients undergoing endoscopic stone surgery is oral pharmacotherapy. The clinical oral standard consists of off-label oral administration of calcium channel blockers, α-blockers or phosphodiesterase inhibitors[11]. Early evidence suggested that oral, systemic-induced relaxation of the ureter results in improvement of stone passage rates[11]. Several recent studies, however, have failed to replicate these findings. Two randomized prospective trials failed to show improvement in stone passage rates for patients with ureteral stones treated with calcium channel or α-blockers[14,15]. Preoperative oral α-blockers have been used in an attempt to reduce sheath insertion forces to improve surgical outcomes[3].

One hypothesis is that the failure of trials to show strong and consistent efficacy with oral calcium channel or α-blockers is due to limitations in oral drug delivery. Calcium channel and α-blockers non-selectively inhibit smooth muscle contraction, which affects the vascular smooth muscle of blood vessels. Dosage is, therefore, limited due to systemic side effects. Delivering systemic doses higher than those currently approved by the U.S. Food and Drug Administration (FDA) would result in dangerous hypotension[16]. Guidelines for administration of these drugs to induce sufficient ureteral relaxation beyond recommended oral doses are not established. Moreover, other therapeutic compounds that also have the potential to induce ureteral relaxation are either currently unavailable as an oral medication or are not FDA-approved[17].

Local delivery of medications for ureteral smooth muscle relaxation represents a promising therapeutic treatment option because it may not be limited by the safe range of drug doses required for systemic oral administration. Theoretically, local therapy using substances that reduce ureteral contraction could allow for delivery of doses directly to the urothelium and ureteral smooth muscle at 10,000 times or greater the dosage that would be tolerated for an oral medication, due to unwanted systemic side effects of vasodilation and hypotension. Previous studies have demonstrated that locally administered intraureteral injection does not result in significant systemic absorption. This was demonstrated in a study which showed that patients who experienced anaphylaxis in response to intravenous contrast imaging agents were not at increased risk for

[1]Harvard-MIT Division of Health Sciences and Technology, Massachusetts Institute of Technology, Cambridge, MA, USA. [2]David H. Koch Institute for Integrative Cancer Research, Massachusetts Institute of Technology, Cambridge, MA, USA. [3]The Barbara K. Ostrom (1978) Bioinformatics and Computing Facility in the Swanson Biotechnology Center, Massachusetts Institute of Technology, Cambridge, MA, USA. [4]Broad Institute of Massachusetts Institute of Technology and Harvard, Cambridge, MA, USA. [5]Department of Urology, Massachusetts General Hospital, Harvard Medical School, Boston, MA, USA. [6]Department of Material Science Engineering, Massachusetts Institute of Technology, Cambridge, MA, USA. *e-mail: mjcima@mit.edu

anaphylactic reactions when those agents were administered locally to the ureter[18,19]. Local delivery of therapeutics for stone disease, ureteral stent symptom relief and facilitation of safe passage of endoscopic instruments during surgery have not been used clinically to date. Our hypothesis is that a local approach is superior to systemic delivery because the urogenital tract has a protective barrier that prevents systemic entry of potentially toxic substances[20]. This suggests that there is a higher safety margin for the same drugs delivered locally within the urogenital system, as opposed to systemic administration. It can be envisioned that drugs could be locally administered as routine office-based or emergency-department procedures (that is, cystoscopy with ureteral catheterization) to facilitate stone passage, relief of ureteral colic and stent pain. Such a procedure may reduce the reliance of patients on surgical intervention (lithotripsy) under general anesthesia or as an adjunct to an endoscopic surgical procedure.

Here we present a series of experiments that demonstrate the following: (1) systematic evaluation of candidate pharmacologic agents for local therapy to relax human ureteral smooth muscle cells, (2) ex vivo evaluation of the efficacy of local therapy using porcine ureters and (3) an in vivo porcine study comparing the efficacy of local therapy to standard oral α-blocker therapy. The results lay the groundwork for a human clinical study using local therapy for patients who could benefit from targeted relaxation of the ureter.

Results

Expression of smooth muscle cell markers in human ureteral smooth muscle cells. Five primary human ureteral smooth muscle (hUSMC) lines were produced de novo from discarded distal ureters obtained from patients undergoing a radical cystectomy. hUSMCs were developed de novo, as no commercially available primary cell lines were available. A pathologist verified the negative tumour margins before intraoperative processing and analysis. hUSMCs were cultured using the de novo technique (Fig. 1a). Characteristic smooth muscle cell phenotypes were observed and verified under microscopy after enrichment and growth (Fig. 1b).

Automated screening and analysis of hUSMCs relaxation in vitro. Eighteen small molecules were used for an automated screen to investigate their effect on local relaxation of human ureteral smooth muscle (Table 1). The small molecules screened included α-adrenoceptor antagonists, β-adrenoceptor agonists, phosphodiesterase inhibitors, calcium channel blockers, nitric oxide donors, Rho-kinase inhibitors (ROCKi), prostanoids and 5-HT3 receptor antagonists. The selected classes of therapeutics were based on previous literature that examined the effects of various molecules on ureteral relaxation in vitro[17].

The in vitro physiological response of contraction and relaxation in hUSMCs can be characterized by quantifying the amount of myosin light chain phosphorylation[21–25]. This approach can thus be adopted to determine relaxation across the hUSMC populations by quantifying the amount of phosphorylation-signal loss after drug treatment via immunofluorescence imaging. hUSMCs were found to basally express a high level of myosin light chain phosphorylation, indicating a baseline contractile state. Loss of this signal indicates a more relaxed state.

hUSMCs were first exposed to individual drugs at 10 μM for 1 h, 2 h, 4 h, 8 h and 24 h time points to optimize the time points for an in vitro readout of relaxation response. The 6 h exposure was determined to be optimal, as further exposure of candidate drugs did not lead to greater decreases in fluorescence. A computer vision segmentation technique using the open-source software CellProfiler was developed to quantify phosphorylation and thus relaxation[26]. The nucleus and cell boundary for each hUSMC was identified (Fig. 2a–d). The integrated fluorescence intensity from each segmented region was determined and averaged across all cells in each drug- or vehicle control-treated sample. Preliminary screens were conducted to determine the rank order of the therapeutics for relaxation effects using three of the unique primary human cell lines. These screens implemented an eight-point dosing curve from 0 μM to 25 μM for all drugs.

Table 1 | Small molecule screen for targeted hUSMC relaxation

Compound	Trade name	Target/Effect
Tamsulosin	*Flomax*	α-adrenoceptor antagonist
Isoproterenol	*Isuprel*	β-adrenoceptor agonist
Butoxamine	–	β-adrenoceptor antagonist
Mirabegron	*Myrbetriq*	β-adrenoceptor agonist
Sildenafil	*Viagra*	PDEI
Vardenafil	*Levitra*	PDEI
Rolipram	–	PDEI
Nifedipine	*Adalat; Procardia*	Calcium channel blocker
Y-27632	–	ROCKi inhibitor
Prostaglandin E1	*Prostin*	Natural product/COX-2 pathway
Prostaglandin E2	*Cervadil; Prepidil*	Natural product/COX-2 pathway
Diclofenac	*Cataflam; Voltaren*	COX-2 inhibitor
Celecoxib	*Celebrex*	COX-2 inhibitor
Ondansetron	*Zofran*	Serotonin 5-HT3 receptor antagonist
Tiotropium	*Spiriva*	Anticholinergic bronchodilator
Adenosine	*Adenocard*	Antiarrhythmic agent
Atropine	*Atropen*	Muscarinic acetylcholine receptor antagonist
L-arginine	–	Nitric oxide pathway

hUSMC primary cell lines were screened in vitro against 18 small molecules. The trade names of compounds are provided where available. Drug classes and putative targets are also presented. These classes of therapeutics were deemed to be relatively encompassing due to contractile physiology of smooth muscle in the human ureter[17]. PDEI, phosphodiesterase inhibitor; COX-2, cyclooxygenase-2.

Compared with a dimethyl sulfoxide (DMSO) vehicle control, the following compounds demonstrated a notable loss of immunofluorescence signal (corresponding to relaxation) in individual cell lines or in average: tamsulosin (17%), vardenafil (18%), tiotropium (15%), celecoxib (17%), ondansetron (16%), prostaglandin E2 (17%), atropine (14%), rolipram (19%) and diclofenac (10%) ($^{*}P \leq 0.05$, Supplementary Fig. 1). Nifedipine and ROCKi yielded the greatest amount of relaxation. Significant loss in the immunofluorescence signal was observed after treatment with nifedipine and ROCKi (Fig. 2g,h) compared with treatment with either the DMSO vehicle control or tamsulosin, which is currently the gold standard for oral dosing (Fig. 2e,f). Nifedipine and ROCKi achieved 35% ($^{*}P \leq 0.05$) and 39% ($^{**}P \leq 0.01$) hUSMC population relaxation, respectively, at the 25 μM upper-bound dose (Supplementary Fig. 1). None of the compounds were significantly cytotoxic, maintaining average cell viability above 83% (Supplementary Fig. 2), with the exception of celecoxib, which led to greater than 60% cell population death at the 25 μM top dose ($^{*}P \leq 0.05$). Nifedipine at concentrations between 50 μM and 100 μM were also found to be cytotoxic; these concentrations were excluded from testing in further screening optimizations.

The two most promising candidates selected from the initial screen to induce hUSMC population relaxation were nifedipine and ROCKi. They were therefore used in further dose-screening assays across all five of the unique primary hUSMC cell lines. Tamsulosin was set as a baseline since it is used as the clinical gold standard

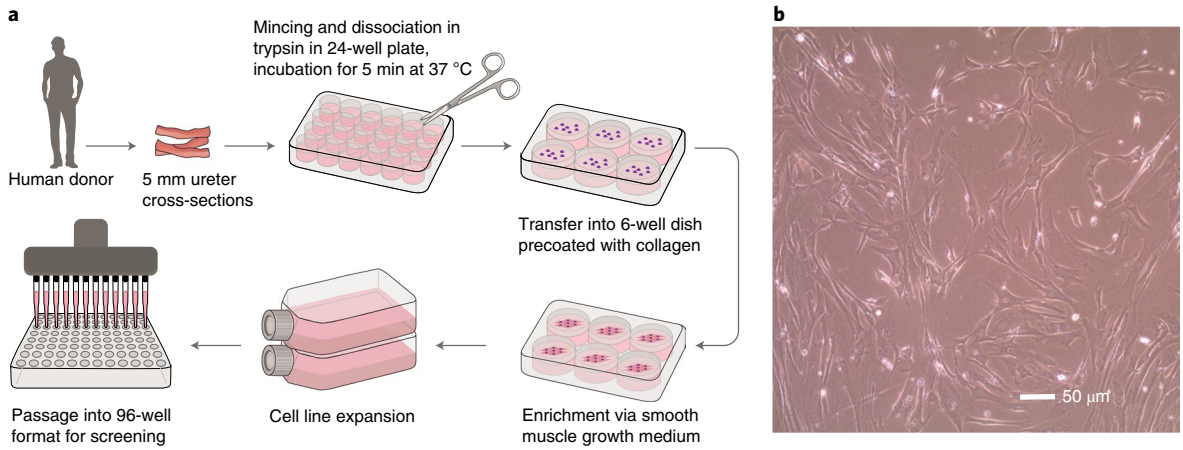

Fig. 1 | Establishing an in vitro model compatible with automated screening. a, Schematic representation of key procedural steps for the growth of primary hUSMCs in vitro. **b**, Light microscopy image of partially confluent hUSMC in vitro resulting from primary cell culture. Image captured using EVOS FL Auto Imaging System (Life Technologies).

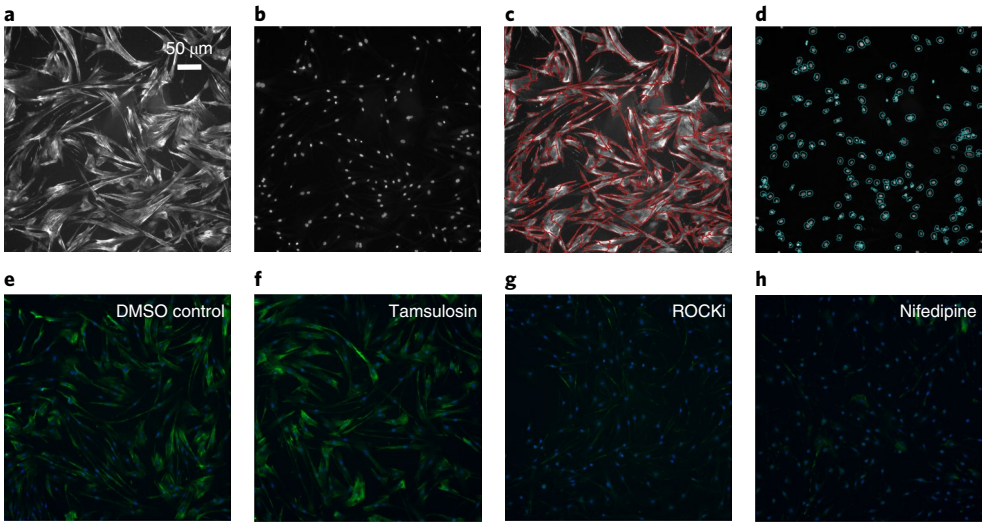

Fig. 2 | Automated screening and single-cell analysis of hUSMC relaxation in vitro. a–**d**, Segmentation and identification of hUSMCs. **a**, Characteristic greyscale image from an automated screening content imager stained with anti-diphospho-myosin light chain antibody. **b**, Characteristic greyscale image from an automated screening content imager stained with Hoescht stain for cell nuclei. The view is identical to (**a**). **c**, Implementation of the CellProfiler segmentation algorithm to detect and delineate hUSMC cells. This view is identical to (**a**), but computer-vision regions corresponding to hUSMCs were segmented and outlined in red. **d**, Implementation of the CellProfiler segmentation algorithm for detection of cell nuclei. This view is identical to (**b**), but computer-vision regions corresponding to hUSMC nuclei were segmented and outlined in cyan. **e**–**h**, In vitro relaxation observed after exposure to key drug candidates at the 25 µM top dose. Green corresponds to the anti-diphospho-myosin light chain; blue corresponds to the Hoescht stain. **e**, A representative image of vehicle-treated hUSMC fluorescence in vitro. **f**, A representative image of hUSMCs after exposure to 25 µM tamsulosin (the oral gold standard). No significant loss of green signal is observed. **g**,**h**, Representative images of hUSMCs after exposure to 25 µM ROCKi and 25 µM nifedipine, respectively. Significant loss of green signal is observed in hUSMCs treated with nifedipine and ROCKi compared with the DMSO control and tamsulosin. The scale bar in (**a**) applies to all images in (**a**–**h**).

for oral therapy. Nifedipine and ROCKi were confirmed effective hUSMC relaxation agents, resulting in a maximum average cell population relaxation of 44% and 42% (***$P=0.0006$, ***$P=0.0003$) at a 25 µM maximum dose, respectively (Fig. 3a,b). Tamsulosin was effective in only a single patient cell line (up to 29% relaxation), but with no overall significant effect when averaged across multiple lines (Fig. 3c). Compared with the equivalent oral tamsulosin dose, nifedipine and ROCKi demonstrated a ten-fold increase in relaxation. Average cell viability was greater than 91% for all doses of nifedipine, ROCKi and tamsulosin (Fig. 3d–f).

Combination in vitro drug screening. A combination drug screen was developed using the two most potent local inhibitors of hUSMC contraction, ROCKi and nifedipine, to quantify the potential for combinatorial drug synergy. Combination treatment was hypothesized to allow in vitro relaxation to be achieved with lower doses of each of the drugs individually. Combination in vitro dosing was conducted on a 10-point nifedipine dose curve (0–50 µM) and an 8-point ROCKi dose curve (0–25 µM, Fig. 4a,b). Screens were conducted across all five unique primary hUSMC lines. Combination drug exposure in vitro compared with single-drug exposure resulted

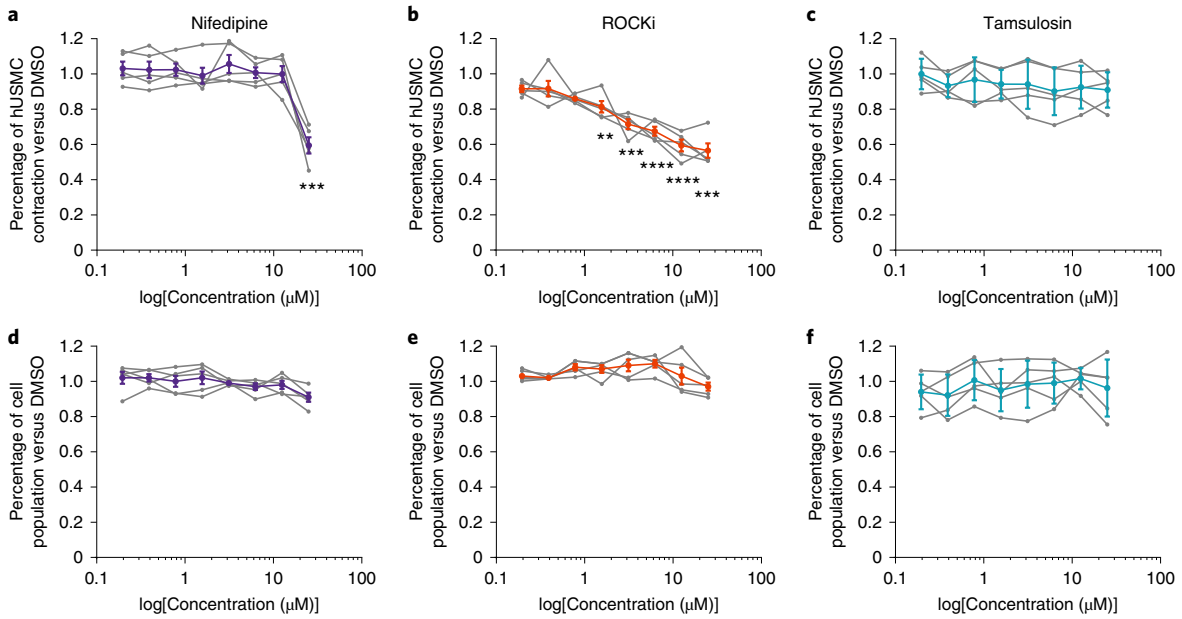

Fig. 3 | In vitro hUSMC relaxation of screened candidates of interest. Five unique primary patient (biological replicates) cell lines were screened (grey), with the means ± s.e.m. displayed in colour. **a**–**c**, Full 8-point dosing curves for nifedipine, ROCKi and tamsulosin. Significant relaxation is incurred with increasing doses of ROCKi (up to 41.6% relaxation at 25 μM, $^{***}P = 0.0003$). Other ROCKi doses exhibited significant differences: $^{****}P \leq 0.0001$, $^{***}P = 0.0002$ and $^{**}P = 0.0030$. At the 25 μM top dose of nifedipine, significant relaxation occurred (43.6% relaxation, $^{***}P = 0.0006$). Tamsulosin was also screened as a comparison with the oral gold standard. Up to 29.1% relaxation was observed in individual cell lines but with no overall statistical significance. **d**–**f**, Percentage cell viability of hUSMC cell populations corresponding to **a**–**c**. Percent cell viability of hUSMCs after treatment with all three drug candidates was at least 91% on average. Statistical significance across all panels, when applicable, was determined using a two-sided Student's *t*-test.

in significantly increased hUSMC relaxation. hUSMC relaxation of 72% ($^{****}P \leq 0.0001$) was observed at the highest combination drug exposure (50 μM with 25 μM of ROCKi and nifedipine) compared with DMSO controls and maximum relaxation induced by either drug administered alone ($^{****}P \leq 0.0001$). Several drug combinations yielded greater than 44% relaxation, which was the maximum relaxation induced by either drug administered individually. Increasing the dose of nifedipine and ROCKi yielded greater in vitro hUSMC relaxation, but doses above 12.5 μM nifedipine and 25 μM ROCKi had no further effects on relaxation. Optimal in vitro dosing was observed for a combined treatment with 12.5 μM nifedipine and 25 μM ROCKi. The safety of the combined drug exposure was verified by observation of in vitro cell viability of at least 87% on average for all conditions including DMSO controls. Comprehensive in vitro combination relaxation data and cell viability are provided in supplemental materials (Supplementary Figs. 3–4).

A nonparametric statistical model conventionally used to detect genes with differential expression under two experimental conditions was adapted for hUSMC relaxation after exposure to two drugs[27]. A unitless, synergy coefficient between −0.5 and +0.5 was calculated from this model (Equation (1)). A coefficient of −0.5 indicates maximum multiplicative drug synergy, whereas a coefficient of +0.5 indicates drug antagonism. A coefficient of zero indicates no synergy. Several combination dosing conditions (including 12.5 μM nifedipine and 25 μM ROCKi) were found to be statistically significant for multiplicative drug synergy ($^{*}P \leq 0.05$) on further analysis with the adapted statistical model (Fig. 4c, Supplementary Fig. 5).

Ex vivo effects and pharmacodynamic assessment. Nifedipine and ROCKi were tested ex vivo to assess pharmacodynamics and translate the findings from in vitro cell-based data to the organ level. Ureteral contractions were stimulated pharmacologically[28] using a bench-top ex vivo system (Fig. 5a). Ureters can be pharmacologically stimulated to repeatedly contract for several hours ex vivo with a 10 μM solution of phenylephrine in Krebs-Henseleit Buffer (KHB) (Supplementary Fig. 6). Infusion of this solution before drug exposure allowed each sample to serve as a baseline control for itself. Nifedipine and ROCKi solutions were delivered intraluminally to ex vivo ureters individually as follows: each ureter was first exposed to 10 μM phenylephrine to establish a baseline for each sample, followed by 25 μM nifedipine or 25 μM ROCKi (concentrations screened to be effective in vitro, all instilled at 0.5 ml min^{-1}). The intraluminal pressure waveforms were measured using a 0.9 F fiber-optic pressure transducer (Fig. 5b). Cumulative contractions were quantified and plotted against time. Representative figs. displaying cumulative contractions over the course of intraluminal nifedipine or ROCKi infusion are provided (Fig. 5c,d). An infusion of 25 μM nifedipine resulted in cessation of peristatic ureteral contractions compared with infusion of the phenylephrine control (Fig. 5c), and 25 μM ROCKi resulted in a 2.5-fold decrease in peristaltic ureteral contractions compared with the control (Fig. 5d). Baseline ureteral contractions were observed after flushing nifedipine or ROCKi from the ureters. These experiments demonstrated that infusion of KHB with nifedipine or with ROCKi resulted in complete elimination or reduction of ureteral contractions, respectively. The effects of intraluminal drug delivery could be reversed pharmacologically, which was observed (demonstrating a favourable safety profile). These findings confirm that ROCKi and nifedipine are viable candidates for local delivery.

Drug exposure was increased by compounding nifedipine and ROCKi into a lubricant for local delivery. Sterile, off-the-shelf, FDA-approved surgical lubricant was used as a matrix to compound with the drug and deploy it directly into the ureter. Surgical lubricant was selected because these types of lubricants are commonly used to facilitate the passage of endoscopes and instruments into the urinary tract[29]. Initial testing demonstrated that even with

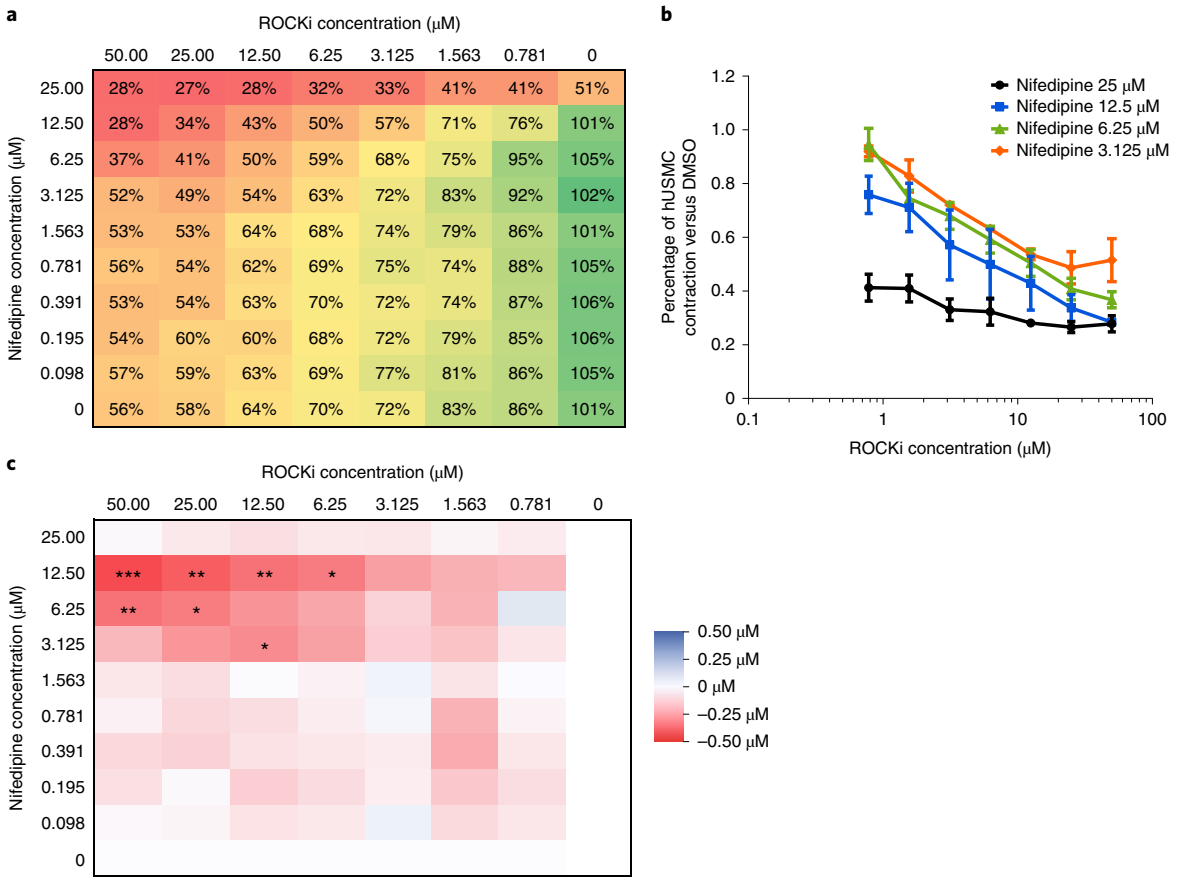

Fig. 4 | In vitro hUSMC relaxation synergies from combination doses of lead drug candidates, nifedipine and ROCKi. Figures correspond to averages and values obtained from five unique primary (biological replicates) hUSMC cell lines. **a**, Average percentage of hUSMC cell populations across different ranges of ROCKi and nifedipine concentrations that remain contracted. 72% relaxation (****$P \leq 0.0001$) was observed at the highest drug concentrations. This exceeded relaxation observed after individual drug exposure (~40%). The bottom right corner corresponds to DMSO vehicle control with no drug exposure. Variations in plated hUSMC populations account for percentages exceeding 100%. **b**, In vitro relaxation response curves with fixed nifedipine doses are plotted against varying dosages of ROCKi. Only response curves with statistically significant drug synergy are presented. All values above 6.25 μM ROCKi are significant for reducing percentage hUSMC contraction when compared with DMSO vehicle control (at least ***$P \leq 0.001$). Data are means ± s.e.m. **c**, Adaptation of a nonparametric statistical model for two experimental conditions applied to determine multiplicative drug synergy across all combination dosing conditions. Several conditions were found to be statistically significant for multiplicative drug synergy (from left to right, top to bottom: ***$P = 0.0005$, **$P = 0.0023$, **$P = 0.0090$, *$P = 0.017$, **$P = 0.0094$, *$P = 0.017$ and *$P = 0.037$). Additive drug synergy was also calculated and found to corroborate synergy findings (Supplementary Fig. 5). Statistical significance across all panels, when applicable, was determined using a two-sided Student's *t*-test.

homogenous mixing, the simple addition of solubilized drug into surgical lubricant was ineffective in retaining any drug, as nifedipine is practically insoluble in water (Supplementary Fig. 7–8). The US Pharmacopeia Compendium[30] was consulted, and several surfactants commonly used to increase drug solubility were considered. Polysorbate 20 was found both to increase drug retention in water-based gels and to provide a generous safety profile as a compounding additive. Varying concentrations of surfactant were tested, but polysorbate 20 volumes exceeding 5% v/v substantially reduced the viscosity of the lubricant. Given the limited quantity of ureters that could be obtained ex vivo, this lubricant formulation was used to increase drug retention within the ureteral lumen for an exposure study. A clinical embodiment comprised of 96% v/v surgical lubricant, 3% v/v polysorbate 20, and 1% nifedipine + ROCKi was formulated for testing ex vivo (Fig. 5e). Quantification using ultraviolet (UV)-absorbance showed that 3% v/v polysorbate 20 allowed surgical lubricant to retain approximately 100 μM and 200 μM of ROCKi and nifedipine, respectively (Supplementary Fig. 9). Cessation of contractions was observed with intraluminal deployment of 5 ml of lubricant containing drugs. Ureters treated with lubricant alone continued to contract (Supplementary Fig. 10). These findings reinforce the results seen with intraluminal infusion of drug solutions (Fig. 5c,d).

Each ureter served as both the experimental condition and its own control, and the quantity of contractions was analysed for discrete five-minute increments corresponding to each experimental condition (Fig. 5f). Intraluminal infusion of nifedipine during these 5 min intervals following drug delivery reduced the median quantity of contractions from 5 contractions per 5 min to 0 contractions (**$P = 0.0036$). Intraluminal infusion of ROCKi reduced median contractions every 5 min from 5 to 2 contractions (**$P = 0.0018$). Flushing the ureters with saline after halting drug infusion led to a return to baseline contractile frequency. This provided confidence that the relaxation effects were attributed to the nifedipine or ROCKi and not death of ureteral smooth muscle cells. Intraluminal delivery for ROCKi- and nifedipine-retained surgical lubricant reduced median contractions from 5 to 0 contractions (****$P \leq 0.0001$). A statistically significant difference was not seen between the median contraction rate of ureters treated with phenylephrine and ureters treated with phenylephrine and lubricant without drug. This

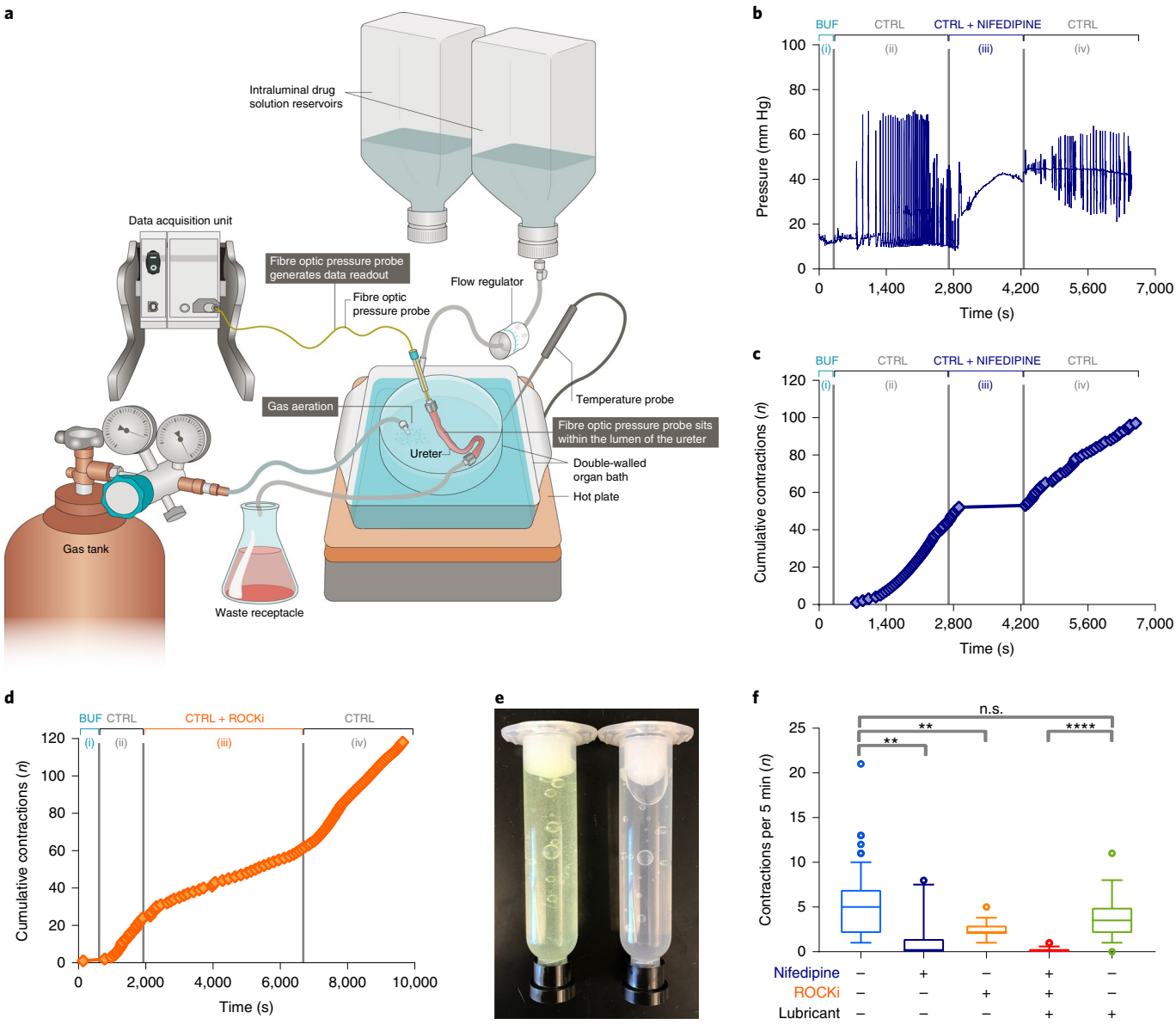

Fig. 5 | Ex vivo validation using porcine ureteral segments. a, Ex vivo bench top model for testing individual ureters. Flow was regulated at 0.5 ml min^{-1}. A mixture of 95% oxygen and 5% carbon dioxide (carbogen) was bubbled through the extraluminal bath, which contained standard KHB heated to 37 °C. The intraluminal reservoirs contained either preheated Krebs buffer (BUF), 10 μM phenylephrine in KHB (CTRL) or 10 μM phenylephrine in KHB with 25 μM ROCKi or 25 μM nifedipine. **b**,**c**, These panels correspond to the same experiment but are provided together for clarity; **b**, The representative waveform obtained from a pig ureter after intraluminal installation of buffer (i), 10 μM phenylephrine (ii) and 10 μM phenylephrine with 25 μM nifedipine (iii). The ureters were then flushed. After flushing, 10 μM phenylephrine was once again delivered (iv). Active nifedipine delivery eliminated contractions. **c**, Individual contractions events (from **b**) plotted as cumulative contractions over time. **d**, Individual contractions events plotted as cumulative contractions over time. This corresponds to intraluminal instillation of 25 μM ROCKi (iii). Active drug delivery reduced frequency of contractions up to 2.5-fold. **e**, Lubricant containing both ROCKi and nifedipine. Lubricant containing drug candidates shown on the left (yellow); lubricant containing no drug is shown on the right (colourless). Supplementary Fig. 10 provides additional plots for cumulative contractions over time with drug and non-drug formulated relaxation responses similar to that shown in (**c**) and (**d**). **f**, For each of the five conditions presented, two ureters were used ex vivo ($n = 2$ biological replicates per condition). Number of contractions for non-overlapping 5-min time intervals corresponding to each condition are totalled and presented. Median number of contractions was reduced from 5 to 0 during nifedipine infusion ($^{**}P = 0.0036$). Median number of contractions was reduced from 5 to 2 during ROCKi infusion ($^{**}P = 0.0018$). Median number of contractions was reduced from 5 to 0 comparing intraluminal delivery of 5 ml lubricant containing no drug to 5 ml lubricant containing the drug ($^{****}P \leq 0.0001$). No statistical significance was observed between ureters treated with only phenylephrine or with phenylephrine and lubricant alone. Box plot shows tails spanning 10–90th percentiles. The Minimum/Q_1/Median/Q_3/Maximum for each condition is as follows (left to right): 1/2/5/7/21; 0/0/0/1.5/8; 1/2/2/3/5; 0/0/0/0/1; 0/2/3.5/5/11. n.s., not significant. Statistical significance across all panels, when applicable, was determined using a two-sided Student's *t*-test.

indicates that the lubricant alone does not elicit any physiological effect. Post-experimental histology showed no clinically significant pathology for all experimental conditions (Supplementary Fig. 11).

Contractions of ex vivo ureters were measured. Amplitudes of ex vivo ureters were not compared because the ureters originated from pig specimens of varying sizes (30–90 kg) at time of death.

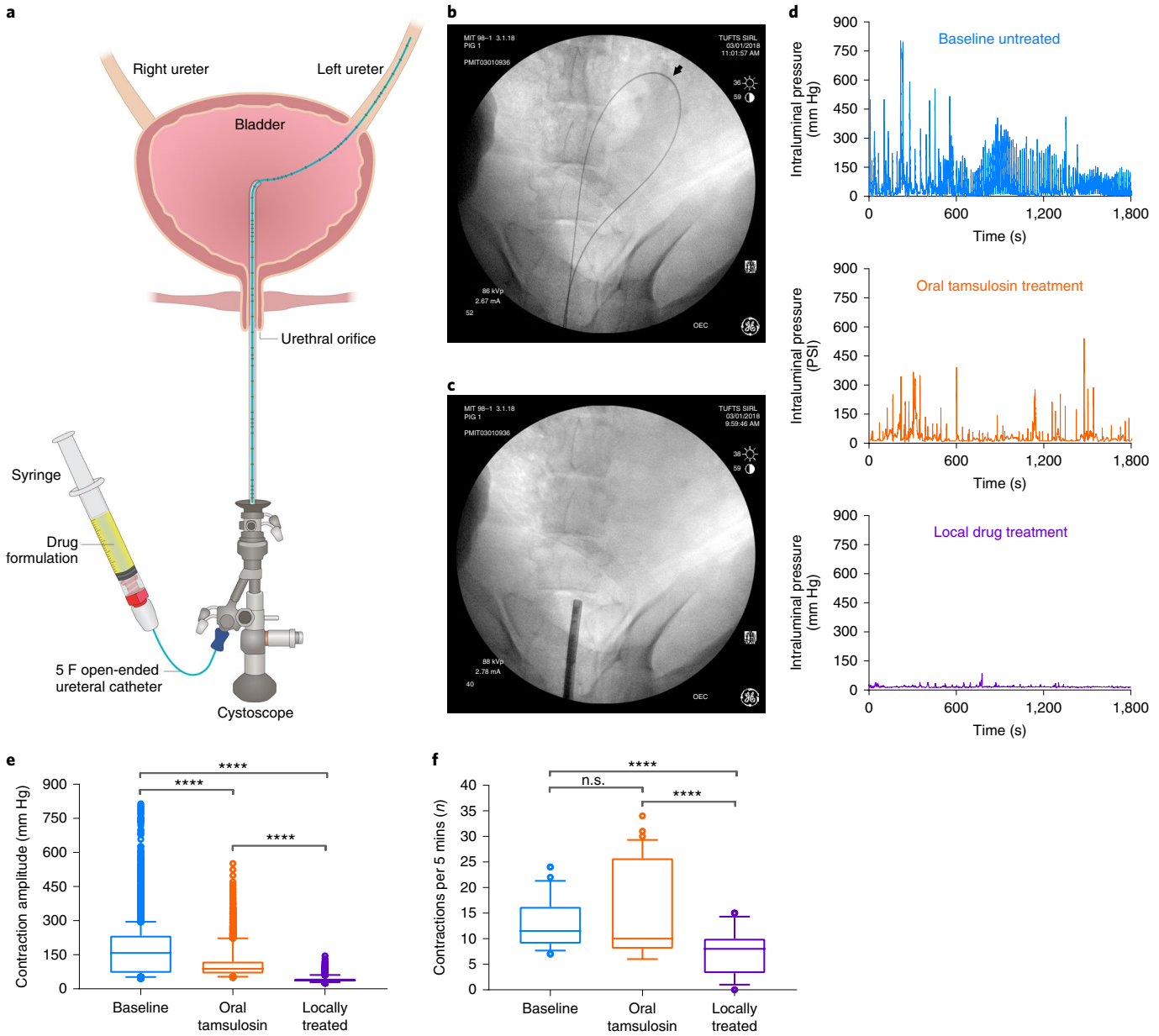

Fig. 6 | In vivo validation of nifedipine and ROCKi. a, The cystoscopic procedure performed in adult female pigs. **b**, Fluoroscopy image showing a radiopaque guidewire (arrow) forming a loop after contact with a kidney calyx. This is visual confirmation for proper catheter introduction into the lumen of the ureter. **c**, Fluoroscopy image with 5 French Units (F) open-ended ureteral catheter deploying drug formulation (not visible, as it is not radiopaque) within lumen of the ureter. **d**, Characteristic peristaltic pressure data recorded from within the lumen of the ureter in mm Hg. Each recording is a continuous waveform representing 30 min of data acquisition from one pig. Local drug delivery (purple) resulted in significant reduction of contraction frequency and contractile amplitude of the ureter compared with baseline (blue) and oral gold standard, tamsulosin (orange). **e**, Contraction amplitude of ureteral contractions combined from all pigs ($n = 3$ biological replicates). Over 90% reduction in amplitude was observed after local treatment (****$P \leq 0.0001$). Data represent consolidated contraction amplitudes obtained from all pigs. The box plot displays tails spanning the 10–90th percentiles. Minimum/Q_1/Median/Q_3/Maximum for each condition is as follows (left to right): 46/70/158/234/814; 51/67/88/120/551; 25/32/37/46/145. **f**, Combined contraction frequency of treatments from all pigs ($n = 3$ biological replicates). There was no statistical significance between oral tamsulosin- and baseline-treated groups. Local treatment reduced frequency by 50% (****$P \leq 0.0001$). Data represents consolidated contraction frequencies obtained from all pigs. Box plot displays tails spanning the 10–90th percentiles. Minimum/Q_1/Median/Q_3/Maximum for each condition is as follows (left to right): 7/9/11.5/16.25/24; 6/8/10/25.75/34; 0/3.25/8/10/15. n.s., not significant. Statistical significance across all panels, when applicable, was determined using a two-sided Student's *t*-test.

Ureters subjected to ex vivo testing were more sensitive to positional discrepancies in placement (for example, if the transducer tip touched the luminal wall, the signal would be dampened compared with recordings directly in the lumen). Frequency of contractions was therefore used for analysis of treatment efficacy.

In vivo validation, testing and toxicity. An in vivo study was designed to further validate the efficacy of local delivery of the most potent combination, nifedipine and ROCKi. Local delivery of nifedipine and ROCKi was compared with orally administered tamsulosin, the clinical gold standard. The lubricant-containing

drug was deployed intraluminally in 5 ml aliquots via a cystoscope and ureteral catheter into 3 pig ureters to examine the effects on ureteral contractions (Fig. 6a). This cystoscopic approach is equivalent to the approach physicians would use in the clinic to deploy the formulation within a human ureter. Fluoroscopy was used to confirm that the positioning and drug deployment was conducted properly (Fig. 6b,c).

Local treatment with nifedipine and ROCKi proved to be highly effective in reducing the frequency and amplitude of ureteral contractions versus the untreated baseline and oral tamsulosin (Fig. 6d). The average relative contraction amplitude was 160 mm Hg at the baseline (that is, the control), 76 mm Hg in pigs administered with oral tamsulosin and 20 mm Hg in pigs treated locally. (****$P \leq 0.0001$ for comparison of control to tamsulosin, ****$P \leq 0.0001$ for comparison of local treatment compared with either oral tamsulosin or the baseline control Fig. 6e). Frequency of ureteral contractions was not different between baseline control and oral tamsulosin (12 and 11 contractions per 5 min, respectively, P = n.s.), whereas local treatment significantly reduced the frequency of ureteral contractions to 7 contractions per 5 min (****$P \leq 0.0001$ compared with the control and tamsulosin), Fig. 6f.

Serum creatinine did not change with local delivery of nifedipine and ROCKi. All serum creatinine levels pre- and post-treatment were within normal limits (nl: 0.8–2.3 mg dl^{-1}, Supplementary Fig. 12). Minimal to undetectable systemic drug absorption was confirmed via liquid chromatography mass-spectroscopy (LCMS) of serum samples. LCMS quantitated the average serum ROCKi concentration at 0.003 μg ml^{-1} and nifedipine at 0.017 μg ml^{-1} (Supplementary Fig. 13). In comparison, low oral dosing of 10 mg of oral nifedipine yields a peak blood serum concentration of around 0.160 μg ml^{-1} (ref. [31]). Local delivery resulted in a 10-fold decrease from this value, indicating that little to no drug was systemically absorbed. Intraoperative monitoring of vitals also showed no changes after local delivery. Postmortem histopathology revealed no histologic changes in pigs treated with local therapy (Supplementary Figs. 14 and 15).

Discussion

The current study identifies therapeutic agents that can be locally delivered, which resulted in significant decreases in the frequency and amplitude of ureteral contractions compared with placebo and standard oral therapy (tamsulosin). These findings have substantial implications for the treatment of patients with ureteral colic, ureteral stents, ureteral stones or for those who have undergone surgical treatment for ureteral stones. A theoretical advantage of local therapies is that they are applied directly to the target tissue, allowing for higher local effective doses of drugs to be utilized that could not be reached when administered orally, while the risk of systemic side effects is considerably reduced. Therefore, application of local relaxants to the ureter has the potential to create a greater therapeutic effect than the current standard-of-care α-blockers, as local therapy can be applied in doses of greater than 10,000 times when compared with the threshold of tolerance from oral medications.

There are several notable findings from this study. Two compounds, nifedipine and ROCKi, were identified as highly effective in relaxing ureteral smooth muscle. Nifedipine, a calcium channel-blocker used to treat hypertension, carries the risk of hypotension as a side effect if administered at the high systemic oral doses required to induce significant ureteral smooth muscle relaxation. Rho-kinase inhibitors are not currently available as an oral therapy, despite their well-established role in the smooth muscle relaxation pathway[32]. These findings also provide an explanation for recent data demonstrating that oral tamsulosin has poor efficacy (at best) in increasing the spontaneous passage rate of ureteral stones. Emergency physicians, primary care physicians and urologists have used tamsulosin for at least 15 years to help stone passage[33]. This is partly because it is a medication that physicians are familiar with, as it has had long-standing FDA-approval for the treatment of another urologic condition, benign prostatic hyperplasia. The side effect profile at its human clinical dose (that is, 0.4 mg) is low, but so is the efficacy. The in vitro studies, which failed to identify tamsulosin as one of the top three most potent ureteral smooth muscle relaxants, and whose effects were limited to only a subset of patients out of five tested, are consistent with the disappointing findings of the recent randomized trials[34]. The in vitro studies also reveal that meaningful relaxation can be induced with micromolar concentration ranges of drugs, if administered locally (Fig. 3). This confirms the initial hypothesis that insufficient dosing in the ureter is related to ineffective oral therapeutic outcomes. Oral administration of non-specific vasodilators does not yield micromolar dosages at the site of ureteral smooth muscle[35].

Another important finding is the dose-response curve and synergistic effect of nifedipine and Rho-kinase inhibitors in the inhibition of ureteral smooth muscle contraction. Comprehensive experiments were not only able to identify two individual compounds that led to efficient relaxation of the ureter, but also revealed that combinatorial doses optimize this therapeutic effect. Treatment with two drugs simultaneously and quantification of their ureteral relaxation capabilities have not previously been conducted.

These findings have the potential to benefit a large number of patients, as nephrolithiasis alone is a common disease, with a 10% lifetime prevalence globally and an annual incidence of 1% of all Americans aged 18 to 65 (refs. [8,36]). Applying a local therapy that can relax the smooth muscle of the ureter, reduce pain and hasten the time to stone passage will result in improvement in quality of life, reduced emergency department visits and fewer absences from work. The results allow for potential treatment of patients with locally delivered therapy of the ureter in the outpatient setting. It has been shown that flexible cystoscopy with catheterization of the ureter (the procedure to deliver the local agent) is safely performed using local anesthesia with a success rate over 95%[37].

Another potential application for this formulation is for ureteral stenting. Roughly 12% of all stone patients will undergo an endoscopic surgical treatment that almost universally ends with the placement of a ureteral stent to promote drainage of the kidney and healing of the ureter for one to two weeks[37]. These ureteral stents, although they promote drainage of the kidney, cause significant irritation and pain for patients. Current clinical guidelines promote relaxation of the ureter as the mainstay treatment for this group of patients who have an indwelling ureteral stent[10,38]. Surgeons can be envisioned providing a dose of local therapy at the end of these procedures as well to decrease the patients' pain associated with surgery and ureteral stents. Further recent evidence for the role of ureteral relaxation in surgery is data that demonstrates that oral α-blockers facilitate the safe introduction of endoscopes and devices used during endoscopic stone surgery. Considering the significant advantage of local therapy over oral tamsulosin demonstrated in the pig studies presented here, local therapy has the potential to surpass tamsulosin in terms of its ability to facilitate the introduction of instruments and could gain popularity amongst surgeons for routine usage[3].

There remain some limitations to the drug formulation in its current form that require resolution before its full translation to the clinical setting. Confirmation of translation to humans is of course the most prominent. Human clinical studies are warranted before patient administration, but the results provide firm evidence that local drug delivery for human ureteral relaxation is possible. The histopathological data and minimal serum drug concentrations as measured by LCMS also provide confidence that systemic distribution of drug will be minimal. The results, however, presently only demonstrate acute ureteral relaxation of the distal ureter. The current

embodiment is more readily applicable for relieving ureteral colic attributed to stent pain and dilation of the ureter prior to passage of surgical tools during ureteroscopy. Duration of action studies, as well as further understanding of the relaxation effect in the medial and proximal ureter are potentially needed to extend and maximize the relaxation effect for stone passage. Quantification of the maximum in vivo tolerated dose also should be conducted.

Methods

Study design. This study is comprised of several components. First, de novo primary human ureteral smooth muscle cell lines for in vitro testing were developed. Automated screening and single-cell analysis techniques were applied via computer vision to determine which of the several potential drug candidates was the most appropriate for ureteral relaxation. This led to identification of two lead compounds. Synergy was also discovered when the two lead compounds were delivered together, providing greater ureteral relaxation than either drug individually. The two lead drug candidates were subsequently tested together ex vivo, which demonstrated that ureteral relaxation at the organ level could be induced and reversed through pharmacologics. Using off-the-shelf, FDA-approved components, a suitable lubricant containing both lead drug candidates was engineered for local drug retention and deployment in a clinically usable format. The candidate drugs were ultimately validated in vivo by locally delivering a drug-lubricant matrix containing the screened drug candidates into the ureters of pigs. The results of therapeutic administration were compared with the current standard of care (oral tamsulosin) for inducing ureteral relaxation and found to be significantly superior.

Preparation and culture of primary hUSMCs. Commercial hUSMC cell lines are not available. Fresh human ureters were instead obtained from patients undergoing radical cystectomies at Massachusetts General Hospital directly from the operating room. Intraoperative frozen sections were obtained on proximal and distal ureter margins to verify healthy tissue. An attending pathologist confirmed negative margins before culturing tissue segments into primary cell lines. Human ureter retrieval for this study is covered under the MIT Committee on the Use of Humans as Experimental Subjects protocol #1508154982. Each distal ureter was approximately 2 cm in length and maintained in 0.5 l of KHB with 1% Penicillin-Streptomycin (Corning) chilled on ice to ~4 °C until the time of use. Each human ureter sample was used within 90 min of harvesting. The ureter segments were cleaned with a #10 blade and ridded of excess fat and blood. Each segment was then dissected into small 5 mm cross-sections and transferred to individual wells of a 24-well plate (Greiner Bio-One) containing 0.6 ml of 0.25% Trypsin-EDTA (Life Technologies). The dissected segments within each well were macerated using sterile Metzenbaum scissors for 60–90 s or until the tissue could not be sheared further. The plate with the macerated tissue was incubated for 5 min at 37 °C to promote tissue dissociation. Separately, a 6-well plate (Greiner Bio-One) was pre-treated with 200 μg ml^{-1} rat-tail collagen I (Thermo Fisher Scientific) and incubated at room temperature for at least 60 min. This collagen-coated plate was subsequently washed twice with 1 × PBS (Corning). 3 ml of SmGM2 complete cell media (Lonza, #CC-3182) containing 1% Penicillin-Streptomycin was added to each well. The macerated tissue was distributed evenly into all 6 wells for a final growth media to trypsin ratio of 10:1 v/v. Plugged borosilicate glass pipettes were sterilized and used to transfer the trypsinized tissue, as standard polystyrene serological pipettes were found to adhere to the samples.

Each primary hUSMC sample required 3–5 d to adhere to the collagen coated plates. The first media change was performed at 48 h to remove floating tissue chunks that did not adhere to the plate. Subsequently, media changes were performed every 48–72 h. On confluence (~7–10 d after initial plating), the cells were trypsinized and expanded into collagen-coated flasks. The smooth muscle morphology improved after the cells were passaged from the initial 6-well dish. Aliquots of each human patient cell line were frozen in pure fetal bovine serum with 10% DMSO at −80 °C.

Automated screening and imaging of drug targets. *Single drug screen and 96-well plate preparation.* hUSMCs were plated in 96-well, black, clear-bottom plates coated with 200 μg ml^{-1} rat-tail collagen I for at least 1 hr. The plates were washed with 1 × PBS. The cells were plated at an initial density of 10,000 cells per well (±5%) in a volume of 100 μl of complete media. When cells reached ~ 80% confluency (about 2–4 d post-plating), they were treated with a panel of small molecule drugs (Table 1). The drugs were dissolved in DMSO and transferred onto the cells using a 100 nl pin transfer tool (V&P Scientific) mounted on the MCA96 head of a Freedom Evo 150 (Tecan) liquid handler. Each drug was tested in an 8-point dose curve between 1 nM and 25 μM and DMSO was used as a vehicle control. The cells were incubated for the desired dosing time point, usually 6 hr, at 37 °C and 5% CO_2. Media was aspirated off the cells using an EL406 plate washer (BioTek), and cells were treated with 4% PFA+0.5% Triton X-100 to fix and permeabilize them. Cells were washed three times with 1 × PBS+0.05% Triton X-100 (wash buffer), using the plate washer, then blocked with 10% (v/v goat serum and 1% w/v bovine serum albumin in PBS for 20 min at room temperature. The blocking solution was aspirated and anti-diphospho-myosin light chain antibody (Cell Signaling Technologies) was applied at 1:100 dilution in fresh blocking solution. The most robust signal was obtained after incubating the cells with the primary antibody for at least 3 d at 4 °C. The cells were washed after this incubation period 3 times with wash buffer, and secondary antibody, anti-rabbit-AlexaFlour 488 (Thermo Fisher) was applied at a 1:1000 dilution in PBS and incubated overnight at 4 °C. After washing 3 times with wash buffer, cell nuclei were stained with Hoechst 33342 (Thermo Fisher) at a concentration of 10 μg ml^{-1} in PBS for 5 min at room temperature. The cells were washed 3 more times in wash buffer, PBS was added to each well and the plates were sealed using an Agilent PlateLoc. The cells were imaged for fluorescence and montaged using an ArrayScan VTI High Content Imager (Cellomics).

Combination drug screen. For combination drug screening, two separate 96-well compound plates were created, one containing Y-27632 in an 8-point dose curve in each column (0–50 μM) and the other containing nifedipine in a 10-pt dose curve in each row (0–25 μM). Eight DMSO vehicle controls were added to each plate. hUSMCs were plated as described above and grown to ~80% confluency. The two compound plates were pin-transferred into each hUSMC cell plate and incubated for 6 hr. The cells were fixed and stained as described above before they were imaged on the ArrayScan imager.

Drug preparations. 100 mM stock solutions of all screened compounds were prepared in individual, sterile amber vials. All stock solutions were dissolved in sterile DMSO, except L-arginine, which was solubilized using dH_2O, due to solubility constraints. Sterile cell-culture grade DMSO, tamsulosin hydrochloride, nifedipine, isoproterenol, butoxamine, adenosine and L-arginine were obtained from Sigma Aldrich. PGE1, PGE2, rolipram, L-arginine, ondansetron, celecoxib, diclofenac, mirabegron, sildenafil, atropine, vardenafil and tiotropium were obtained from Cayman Chemical. Y-27632 dihydrochloride was obtained from R&D Systems. Stock solutions when unused were stored at −20 °C

Verification of smooth muscle phenotype. To verify the smooth muscle phenotype, hUSMCs were plated at 10,000 cells per well in 96-well collagen coated plates and grown to confluency, as above. Cells were fixed and stained for nuclei (using the Hoechst stain), di-phospho-myosin light chain and actin as a smooth muscle marker. They were also stained for MyoD, a marker for skeletal muscle and no signal was seen.

Preparation of ex vivo whole porcine ureters. Whole porcine ureters were obtained through discarded tissue exchange agreements from other IACUC-approved research protocols (MIT protocol #CIMA-E14–08–0617), which would have otherwise been discarded as waste. No pigs were procured solely for ex vivo testing. Whole porcine ureters were obtained from pigs of varying sizes (30–80 kg, *Sus scrofa domesticus*) used for non-urological research immediately after euthanasia. The ureters were obtained from either Tufts Surgical Research or CBSET, Inc. Each ureter was transported in 1 l KHB buffer containing 10 ml of 100 × Penicillin-Streptomycin chilled on ice to ~4 °C and used within the hour. Each ureter was cleaned, dissected of fat and connective tissue and rinsed with KHB-solution to wash away residual blood. Ureters incapable of being pharmacologically stimulated via phenylephrine were discarded.

Ex vivo organ system. A bench top ex vivo system that allows the testing of whole ureteral segments was adapted for use within the Cima Lab[28]. This ex vivo system enables the testing of freshly harvested ureteral segments. The system consists of a double-walled extraluminal organ bath heated to 37 °C. The ureteral segments are placed in the heated organ bath comprised of KHB (Sigma Aldrich). This ex vivo model also provides ureteral segment aeration, as 'capillary gas exchange', which can be implemented by continuously bubbling a mixture of 95% O_2 and 5% CO_2 (Airgas) through the extraluminal bath. Ureteral contractions are stimulated pharmacologically ex vivo, as stones cannot be physiologically replicated. Drug solutions were separately prepared for intraluminal instillation. To stimulate contractions similar to a ureteral obstruction from a stone, a 10 μM solution of phenylephrine in KHB is used as control. 100 mM ROCKi and nifedipine stock solutions were made in DMSO and spiked into the 10 μM phenylephrine for intraluminal drug instillation. Drug flow into the ureters was regulated through gravity-driven flow-regulators (Wolf Medical Supply, RF2500). Properly prepared (see previous section) ureters were cannulated on both sides using a female-luer to male-barbed adapter (McMaster-Carr, #51525K121), and tied off using surgical suture (Ethicon PERMA-HAND). One end of the ureter was connected to the flow regulator and the other end was connected to piping for waste collection. Ex vivo intraluminal pressure readings are obtained through a 0.9 F fiber-optic catheter at 10 Hz (FISO Life-Sciences, Product #750706). The probe was introduced via the drug infusion port of the flow regulator. Experimental runs that used lubricant were also initiated in the same manner. 10 μM of phenylephrine was instilled to pharmacologically stimulate the ureters ex vivo as a control. 5 ml of lubricant (both formulated with drug and without drug) was deployed intraluminally. Deployment was achieved by briefly disconnecting the proximal end from the

waste piping to allow the lubricant to rest within the ureter. Flow to waste was then reconnected.

Drug lubricant formulation. Surgilube was obtained from Medline. Y-27632 hydrochloride was obtained from LC Laboratories (Woburn, MA). Nifedipine and polysorbate 20 were obtained from Sigma Aldrich. Creation of the drug-lubricant combination required 19.4 ml of lubricant and 0.6 ml of polysorbate 20. Separately, 1 M stock solutions of nifedipine and ROCKi were solubilized in DMSO and vortexed within a standard Eppendorf. 100 µl of each stock solution was added to 20 ml of the lubricant-surfactant mixture, for a final concentration of 10 mM, and mixed in a centrifugal speedmixer (FlackTek, Inc.) at 2,150 rpm for 60 s.

A technique was developed to quantify drug concentration within the lubricant using UV-absorbance. Aliquots of lubricant formulations after speedmixing were transferred into a standard Eppendorf. The Eppendorf was then centrifuged at 13,000 rpm for 10 mins. The same was performed for control lubricant formulations, which did not contain any drug. The goal of high-speed centrifugation was to quantify the amount of drug the lubricant itself could capture and retain. An increase in drug retention and decrease in drug precipitate was observed with increasing amounts of polysorbate 20. A small sample of the solid supernatant layer of the drug-lubricant or control-lubricant was extracted into a new Eppendorf and was weighed. Saline was added to each sample at a 15:1 volume to weight ratio, making the sample more soluble and to dilute the drug to fall within the standard curve dose range. Separately, ROCKi and nifedipine standard curves were created by diluting the above 1 M stocks into saline to 200 µM and serial-diluting 2-fold for 12 points. 100 µl samples of the standard curve, control, and experimental samples were then loaded into a 96-well clear UV-transparent plate (UV-Star, Grenier Bio-One) and the absorbance was read using a Tecan M1000 Infinite Pro plate reader at both 230 nm for nifedipine and 270 nm for ROCKi. The concentration of each drug retained in the lubricant-surfactant mixture was calculated from the linear equations for each drug from the standard curves.

Automated screening image analysis. CellProfiler was used to perform image analysis and acquire individual hUSMC fluorescence values[26]; a complete pipeline to replicate analysis is provided as Supplemental Information. In brief, grayscale images obtained from automated screening were segmented for nuclei and hUSMC cell borders. Nuclei were typically 6–30 pixel units in diameter. Each individual well from the 96-well plates produced 9 two-channel images. 18 images were therefore processed for each well (corresponding to nuclei and phospho-myosin light chain). A three-class Otsu thresholding method was applied to the hUSMCs. Across all 9 fields of view, the integrated intensity of all identified and segmented hUSMCs was calculated. Likewise, across all 9 views, the number of identified cell nuclei was summed and calculated (cell count). Repeating this across all 96-wells yields an integrated intensity value and a total viable hUSMC cell count for each well. These values can then be readily analysed for relaxation effectiveness and toxicity. Given the scale of the experiment, all computation was conducted in the cloud using Amazon Web Services. Over 900 million individual cells were analysed.

Statistical analysis of automated screening. Data for both initial screening and single drug screening runs are presented as means ± s.e.m. unless otherwise specified. Comparisons are conducted using Student's *t*-test unless otherwise specified, with significant differences defined as $^{*}P \leq 0.05$, $^{**}P \leq 0.01$, $^{***}P \leq 0.01$ and $^{****}P \leq 0.001$. For drug synergy calculations and comparisons, see the following sections. Variations in plated hUSMC populations account for percentages exceeding 100%. Each individual well screened was divided by the average intensity of all of the DMSO control wells implemented within the run. Therefore, an individual well may have an integrated intensity value slightly above the average integrated intensity value of all DMSO vehicle controls. The resulting calculation of percentage intensity change provides a value that exceeds 100%, which is thus attributed to variations in the cell populations plated. All data figures were visualized using GraphPad Prism v.7 (GraphPad Software). Schematic figures were created using Adobe Illustrator.

Drug synergy analysis. A nonparametric statistical model was adapted[27] to calculate the additive and multiplicative effects of combination drug synergy in this experiment using Equations (1) and (2), respectively.

$$Y_{i,j} = X_{i,j} + 1 - X_{i,0} - X_{0,j} \quad (1)$$

$$Z_{i,j} = X_{i,j} - X_{i,0} \times X_{0,j} \quad (2)$$

Indices i and j correspond to different concentrations of drug A and B, (A represents nifedipine and B represent ROCKi). $X_{i,j} = I_{i,j}/I_{0,0}$ represents the ratio of integrated hUSMCs intensity within a well containing drug (of concentration $A = i$, $B = j$) and a control well with no drug. For equation (1), Y scores the additive combined relaxation of i (ROCKi) and j (nifedipine), while Z scores the multiplicative combined relaxation of i (ROCKi) and j (nifedipine). X represents individual drug concentrations, with $X_{0,0}$ corresponding to DMSO vehicle control.

The same experiment was repeated 5 times. To account for experimental variance, the additive and multiplicative scores for quantifying drug synergy were revised into the following Equations (3) and (4):

$$Y_{i,j} = \frac{\bar{X}_{i,j} + 1 - \bar{X}_{i,0} - \bar{X}_{0,j}}{\sqrt{V_{i,j} + V_{i,0} + V_{0,j}}} \quad (3)$$

$$Z_{i,j} = \frac{\bar{X}_{i,j} - \bar{X}_{i,0} \times \bar{X}_{0,j}}{\sqrt{V_{i,j} + V_{i,0} \times V_{0,j} + V_{i,0} \times \bar{X}^2_{0,j} + V_{0,j} \times \bar{X}^2_{i,0}}} \quad (4)$$

where $\bar{X}_{i,j}$ is the average of $X_{i,j}$ across the experimental replicates, while $V_{i,j}$ is the corresponding variance.

Dose combinations where hUSMCs displayed significant relaxation in response to combination drug treatment was of interest. This scenario provided results in which a lower than expected integrated intensity measurement was seen when compared with the individual relaxation effect from single drug treatment. The stronger the drug synergy, therefore, the lower the synergy score. Conversely, a highly positive synergy score indicates the loss of such drug synergy.

The resulting calculation leads to a unitless value between −0.5 and + 0.5. Values closer to −0.5 indicate high drug synergy, while values closer to + 0.5 represent antagonism. Zero represents no drug synergy. Both additive and multiplicative scores are zero when the concentration of either drug is zero.

Statistical analysis of drug synergy values. The basic assumption underlying the statistics of drug synergy is the null distribution of the additive or multiplicative scores $t = Y$ or Z. The simplest model is one where the distribution of synergy scores follows a Normal distribution $f(t; \mu_t, \sigma_t)$ with mean $\mu_t = 0$ and standard deviation σ_t. Type 1 error is then given by equation (5):

$$\alpha = \int_{cut-off} f(t; \mu_t, \sigma_t) dt \quad (5)$$

Using equation (5), the cut-off value for t can be determined. The *P*-values for drug synergy scores correspond to the probability under which the null hypothesis that an experimental result with a score of less than, or the same as, a result observed is due to chance. This is calculated from the cumulative standard normal distribution given by equation (6).

$$P(Z \leq z) = \int_{-\infty}^{z} f(t, \mu_t, \sigma_t) dt \quad (6)$$

For each synergy score Z, a corresponding *P*-value = $P(Z \leq z)$ was obtained with significant differences defined by $^{*}P \leq 0.05$, $^{**}P \leq 0.01$, $^{***}P \leq 0.001$ and $^{****}P \leq 0.0001$.

In vivo pig surgery. Three adult (70 kg) female domestic swine (*Sus scrofa*) were obtained for in vivo testing. Each pig was provided with two treatments, one week apart. Ureteral contractions were measured after pigs were provided with oral tamsulosin, and on a separate day, after receiving the local drug-lubricant treatment. Since ureteral contractions cannot be readily measured in awake pigs, all pigs were sedated in order to quantify the ureteral relaxation response, after receiving the treatment. Pigs were first randomly assigned to receive either oral tamsulosin or local drug treatment between their scheduled surgical days (7 d apart). When oral tamsulosin was provided, each pig was provided with 0.4 mg oral tamsulosin (equivalent to the human adult dose), 5 h before surgery. The 5 h time interval was selected as this corresponds to peak tamsulosin concentrations after metabolism[39]. Ureteral contractions were then measured. When drug-formulated lubricant was delivered, the pigs were anesthetized, and baseline recordings were obtained before the local delivery of drug lubricant. One hour of intraluminal pressure recordings were taken for each condition (that is, oral tamsulosin, baseline and local delivery). Each pig was maintained for another week after the second procedure and then euthanized for histopathological assessment. All pigs at baseline were maintained on identical diets and fluid intake. The surgical procedure was as follows. Each pig was anesthetized with a cocktail of 8 mg kg^{-1} Telazol, 4 mg kg^{-1} Ketamine and 4 mg kg^{-1} Xylazine IM. Pigs were obtained from Tufts Cummings Veterinary Medical Center. The pigs were intubated with a 7 F endotracheal tube and maintained on isoflurane after anesthetization. Each pig was prophylactically provided with 1 g cefazolin IV for urinary tract infection. The pigs were positioned in dorsal recumbency with the vulva exposed. The vulva and surrounding perianal tissue were cleaned and scrubbed. The soft tissue of the vulva and vaginal opening were pushed aside and a 17 F rigid cystoscope (Karl-Storz) was inserted into the urethra. The cystoscope was advanced into the bladder, where the urine was allowed to drain (after placement of the ureteral catheter and pressure probe, and before initiation of any recordings, the bladder was thoroughly drained via the cystoscope sheath). The left ureter was catheterized with a 5 F open-ended catheter. A guidewire was passed via the catheter to the kidney. Fluoroscopy was used to confirm that the catheter was indeed in the left ureter, and the guidewire was subsequently removed after positioning the 5 F

catheter at the level of the distal ureter 2–3 cm proximal to the ureterovesical junction. Ureteral pressure recordings were obtained via a 0.9 F fiber optic pressure catheter at 10 Hz passed through the lumen of the 5 F open-ended catheter (FISO Life Sciences). The distal ureter was selected as the site for data collection as the cells used in our in vitro screens were derived from distal ureteral samples. Due to cost constraints related to veterinary staff and surgical time, it was only possible to take recordings from one portion of the ureter, and we further deemed the distal region as most consistent. Blood samples were taken from the right jugular vein for complete blood count (CBC) and chemical analysis. Blood samples were taken from the left jugular vein for LCMS serum chemistry analysis. LCMS samples were only obtained on surgical days when the pigs received a local treatment. Upon conclusion of the surgery, isoflurane was turned off and the pigs were administered a 3 mg kg^{-1} dose of ketoprofen IM for analgesia. The pigs were then extubated and recovered. CBC and chemistry values were analysed by IDEXX Bioresearch. Pig surgery was covered by MIT protocol #CIMA-1117–107-OS and Tufts School of Medicine protocol #B2017–114.

Quantification of Y-23762 and nifedipine in pig serum using LCMS. 10 ml of pig blood was collected 1 h after local drug delivery from each pig specimen in lithium heparin coated Vacutainers (Becton Dickinson). Blood samples were centrifuged for 5 min at 2,000*g* at room temperature. The supernatant was transferred into several Eppendorfs for storage and snap-frozen over liquid nitrogen before analysis. Serum samples at the time of analysis were diluted 1:10 in extraction mix (75:25:0.2%, acetonitrile:methanol:formic acid), containing a mixture of 13C-15N labelled amino acids at 500 nM (Cambridge Isotope Laboratories) and nitrendipine[40] (100 nM, Cayman Chemical) as internal standards. Diluted samples were vortexed for 30 min at 4 °C and centrifuged for 10 min at 17,000*g* at 4 °C. The clear supernatant was transferred to LCMS vials. Supernatant from an untreated control animal was used to dilute the standard curve.

Quantitative LCMS analyses of Y-23762 and nifedipine was performed on a Dionex Ultimate 3000 ultra-performance liquid chromatography coupled to a Q-Exactive Orbitrap mass spectrometer (Thermo Fisher) equipped with an Ion Max source and a HESI II probe. External mass calibration was performed using the standard calibration mixture every 7 d. 1 µl of sample was injected onto a SeQuant ZIC-pHILIC 150 × 2.1 mm analytical column equipped with a 2.1 × 20 mm guard column (both 5 mm particle size; EMD Millipore). Buffer A was 20 mM ammonium carbonate, 0.1% ammonium hydroxide; Buffer B was acetonitrile. The column oven and autosampler tray were held at 25 °C and 4 °C, respectively. The chromatographic gradient was run at a flow rate of 0.150 ml min^{-1} as follows: 0–20 min: linear gradient from 80–20% B; 20–20.5 min: linear gradient from 20–80% B; 20.5–28 min: hold at 80% B. The mass spectrometer was operated in full-scan, polarity-switching mode, with the spray voltage set to 3.0 kV, the heated capillary held at 275 °C, and the HESI probe held at 350 °C. The sheath gas flow was set to 40 units, the auxiliary gas flow was set to 15 units, and the sweep gas flow was set to 1 unit. MS data acquisition was performed in a range of m/z = 70–1,000, with the resolution set at 70,000, the AGC target at 1 × 106 and the maximum injection time at 20 millisec. Concentrations of Y-23762 and nifedipine were adjusted using the raw peak areas of the internal standards 13C5–15N-valine and nitrendipine, respectively. Absolute quantification was performed with XCalibur QuanBrowser 2.2 (Thermo Fisher) using a 5 ppm mass tolerance and an external, matrix-matched, standard curve method. The limit of quantitation was determined to be 10 nM for nifedipine and 5 nM for Y-23762. Three blood serum samples were run for each pig.

Statistical analysis of ex vivo and in vivo ureteral pressure profiles. Pressure measurements were recorded at 10 Hz in psi and converted to mm Hg. The raw data obtained from the probe included time-points and corresponding intraluminal ureteral pressure values. The data was imported into MATLAB (Mathworks, Inc., v.R2017b). To standardize the data to relative contractile pressures, 760 mm Hg was subtracted from all recorded values (removing 1 atm equivalent). Contraction peaks were then efficiently identified. Based on ureteral physiology, a ureteral contraction typically ranges from 20 to 80 cm H_2O (ref. [41]), therefore, we only qualified a peak as contraction if it was at least 20 mm Hg. The maximum pressure at each peak was recorded for each qualifying contraction. Amplitude comparisons were conducted using a Student's *t*-test. The resulting analysis yielded a list of contraction amplitudes corresponding to each experimental condition. Data from all in vivo runs were consolidated and analysed together.

The *x*-coordinate for each qualifying contraction was also recorded, which corresponded to a time (in s). Non-overlapping five-minute intervals were defined, and the number of qualifying contractions between each interval was summed for each experimental condition (that is, number of contractions between 0–300 s, 300–600 s and so on). Frequency comparisons were also conducted using Student's *t*-test. For ex vivo ureters, non-overlapping 5 min intervals corresponding to each experimental condition were defined (that is, after instillation of control buffer, after instillation of drug solution and so on). Significant differences for both amplitude and frequency comparisons are defined as $^{*}P \leq 0.05$, $^{**}P \leq 0.01$, $^{***}P \leq 0.001$ and $^{****}P \leq 0.0001$.

Histology. Ureter segments from ex vivo experimentation were cut into 3 mm cross-sections, placed into histology cassettes and immersed in 30 ml of 10% neutral buffered formalin for 24 hr. The segments were then transferred and held in 70% ethanol solution until processing. Tissue segments were processed into paraffin blocks using a VIP 5 Tissue Processor (Sakura Finetek). The blocks were sectioned using a microtome (Leica RM2255) at 4 µm. Hematoxylin and eosin staining was performed using a Varistain Gemini (Thermo Shandon). Formalin, ethanol and reagent grade ethanol were obtained from VWR. Xylene was obtained from Avantik (#RS4050). Hematoxylin (#3801575) and eosin (#3801606) were obtained from Leica Biosystems.

Histology from in vivo studies were processed after animal euthanasia. The left and right kidneys were longitudinally bisected and placed in a container of 10% neutral buffered formalin (10:1 ratio formalin to tissue) with the entire lengths of ureter attached. The formalin was changed after 24 hr. Two transverse sections were taken of each kidney at the renal pelvis. Three sections were taken of each ureter. One section of each ureter was taken 1 cm distal to the renal hilus (proximal ureter), 1 cm proximal to the urinary bladder (distal ureter) and at a midpoint 6 cm distal to the first section (mid ureter). Cassettes were processed on a Microm STP 120 (Thermo Fisher) and embedded in paraffin. Blocks were sectioned using a Microm HM 355 (Thermo Fisher) microtome at 5 µm thickness. Hematoxylin and eosin staining was performed using a Varistain Gemini. Reagents used were from Thermo Fisher and included ethanol Flex 100 (#8101), Flex 95 (#8201), xylene (#6601), hematoxylin (#7211) and eosin (#6766008).

Reporting Summary. Further information on research design is available in the Nature Research Reporting Summary linked to this article.

Data availability

The data supporting the results in this study are available within the paper and its Supplementary Information. The raw datasets generated during the study are available from the corresponding author on reasonable request.

Code availability

The CellProfiler algorithms used for image analysis and for non-parametric drug synergy algorithms are included in the Supplementary Information.

Received: 18 June 2018; Accepted: 15 October 2019;
Published online: 02 December 2019

References

1. Ye, Z. et al. Efficacy and safety of tamsulosin in medical expulsive therapy for distal ureteral stones with renal colic: a multicenter, randomized, double-blind, placebo-controlled trial. *Eur. Urol.* **73**, 385–391 (2018).
2. Tharwat, M., Elsaadany, M. M., Lashin, A. M. & EL-Nahas, A. R. A randomized controlled trial evaluating sildenafil citrate in relieving ureteral stent-related symptoms. *World J. Urol.* **36**, 1877–1881 (2018).
3. Koo, K. C. et al. The impact of preoperative α-adrenergic antagonists on ureteral access sheath insertion force and the upper limit of force required to avoid ureteral mucosal injury: a randomized controlled study. *J. Urol.* **199**, 1622–1630 (2018).
4. Jung, H. U., Jakobsen, J. S., Mortensen, J., Osther, P. J. & Djurhuus, J. C. Irrigation with isoproterenol diminishes increases in pelvic pressure without side-effects during ureterorenoscopy: a randomized controlled study in a porcine model. *Scand. J. Urol. Nephrol.* **42**, 7–11 (2008).
5. Scales, C. D., Smith, A. C., Hanley, J. M. & Saigal, C. S. Prevalence of kidney stones in the United States. *Eur. Urol.* **62**, 160–165 (2012).
6. Trinchieri, A. et al. Increase in the prevalence of symptomatic upper urinary tract stones during the last ten years. *Eur. Urol.* **37**, 23–25 (2000).
7. Chen, Z., Bird, V. & Prosperi, M. The latest prevalence of kidney stones in the US and its trends in different genders. *Ann. Epidemiol.* **27**, 512 (2017).
8. Hollingsworth, J. M. et al. Alpha blockers for treatment of ureteric stones: systematic review and meta-analysis. *BMJ* **355**, i6112 (2016).
9. Sridharan, K. & Sivaramakrishnan, G. Medical expulsive therapy in urolithiasis: a mixed treatment comparison network meta-analysis of randomized controlled clinical trials. *Expert Opin. Pharmacother.* **18**, 1421–1431 (2017).
10. Dellis, A. E. et al. Tamsulosin, solifenacin, and their combination for the treatment of stent-related symptoms: a randomized controlled study. *J. Endourol.* **31**, 100–109 (2017).
11. Hollingsworth, J. M. et al. Medical therapy to facilitate urinary stone passage: a meta-analysis. *Lancet* **368**, 1171–1179 (2006).
12. Dauw, C. A. et al. Expulsive therapy versus early endoscopic stone removal in patients with acute renal colic: a comparison of indirect costs. *J. Urol.* **191**, 673–677 (2014).
13. Rose, J. G. & Gillenwater, J. Y. Pathophysiology of ureteral obstruction. *Am. J. Physiol.* **225**, 830–837 (1973).
14. Pickard, R. et al. Medical expulsive therapy in adults with ureteric colic: a multicentre, randomised, placebo-controlled trial. *Lancet* **386**, 341–349 (2015).

15. Furyk, J. S. et al. Distal ureteric stones and tamsulosin: a double-blind, placebo-controlled, randomized, multicenter trial. *Ann. Emerg. Med.* **67**, 86–95 (2016).
16. Press, Y., Punchik, B. & Freud, T. Orthostatic hypotension and drug therapy in patients at an outpatient comprehensive geriatric assessment unit. *J. Hypertens.* **34**, 351–358 (2016).
17. Canda, A. E., Turna, B., Cinar, G. M. & Nazli, O. Physiology and pharmacology of the human ureter: basis for current and future treatments. *Urol. Int.* **78**, 289–298 (2007).
18. Blackwell, R. H. et al. Incidence of adverse contrast reaction following nonintravenous urinary tract imaging. *Eur. Urol. Focus* **3**, 89–93 (2017).
19. Cochran, S. T., Bomyea, K. & Sayre, J. W. Trends in adverse events after IV administration of contrast media. *AJR Am. J. Roentgenol.* **176**, 1385–1388 (2001).
20. Horsley, H., Dharmasena, D., Malone-Lee, J. & Rohn, J. L. A urine-dependent human urothelial organoid offers a potential alternative to rodent models of infection. *Sci. Rep.* **8**, 1238–1251 (2018).
21. Chen, C.-P. et al. In vivo roles for myosin phosphatase targeting subunit-1 phosphorylation sites T694 and T852 in bladder smooth muscle contraction. *J. Physiol.* **593**, 681–700 (2015).
22. Komatsu, S., Kitazawa, T. & Ikebe, M. Visualization of stimulus-specific heterogeneous activation of individual vascular smooth muscle cells in aortic tissues. *J. Cell. Physiol.* **233**, 434–446 (2018).
23. Monical, P. L., Owens, G. K. & Murphy, R. A. Expression of myosin regulatory light-chain isoforms and regulation of phosphorylation in smooth muscle. *Am. J. Physiol.* **264**, C1466–C1472 (1993).
24. Bhadriraju, K., Elliott, J. T., Nguyen, M. & Plant, A. L. Quantifying myosin light chain phosphorylation in single adherent cells with automated fluorescence microscopy. *BMC Cell Biol.* **8**, 43–55 (2007).
25. Baumann, F. et al. Increasing evidence of mechanical force as a functional regulator in smooth muscle myosin light chain kinase. *eLife* **6**, e26473 (2017).
26. Kamentsky, L. et al. Improved structure, function and compatibility for CellProfiler: modular high-throughput image analysis software. *Bioinformatics* **27**, 1179–1180 (2011).
27. Pan, W., Lin, J. & Le, C. T. A mixture model approach to detecting differentially expressed genes with microarray data. *Funct. Integr. Genomics* **3**, 117–124 (2003).
28. Pick, D. L. et al. First prize: chitosan and the urothelial barrier: effects on ureteral intraluminal drug penetration and peristalsis. *J. Endourol.* **25**, 385–390 (2011).
29. Özel, B. Z., Sun, V., Pahwa, A., Nelken, R. & Dancz, C. E. Randomized controlled trial of 2% lidocaine gel versus water-based lubricant for multi-channel urodynamics. *Int. Urogynecol. J.* **9**, 1297–1302 (2018).
30. Rowe, R.C., Sheskey, P. J., et al. *Handbook of Pharmaceutical Excipients* 4th edn (Pharmaceutical Press, 2004).
31. Raemsch, K. D. & Sommer, J. Pharmacokinetics and metabolism of nifedipine. *Hypertension* **5**, II18–II24 (1983).
32. Shimokawa, H., Sunamura, S. & Satoh, K. RhoA/Rho-Kinase in the cardiovascular system. *Circ. Res.* **118**, 352–366 (2016).
33. Dellabella, M., Milanese, G. & Muzzonigro, G. Efficacy of tamsulosin in the medical management of juxtavesical ureteral stones. *J. Urol.* **170**, 2202–2205 (2003).
34. Pickard, R. et al. Use of drug therapy in the management of symptomatic ureteric stones in hospitalised adults: a multicentre, placebo-controlled, randomised controlled trial and cost-effectiveness analysis of a calcium channel blocker (nifedipine) and an alpha-blocker (tamsulosin) (the SUSPEND trial). *Health Technol. Assess.* **19**, 1–171 (2015).
35. Renwick, A. G. et al. The pharmacokinetics of oral nifedipine-a population study. *Br. J. Clin. Pharmacol.* **25**, 701–708 (1988).
36. Saigal, C. S., Joyce, G. & Timilsina, A. R. Direct and indirect costs of nephrolithiasis in an employed population: opportunity for disease management? *Kidney Int.* **68**, 1808–1814 (2005).
37. Gershman, B., Eisner, B. H., Sheth, S. & Sacco, D. E. Ureteral stenting and retrograde pyelography in the office: clinical outcomes, cost effectiveness, and time savings. *J. Endourol.* **27**, 662–666 (2013).
38. Wang, J. et al. The role of solifenacin, as monotherapy or combination with tamsulosin in ureteral stent-related symptoms: a systematic review and meta-analysis. *World J. Urol.* **35**, 1669–1680 (2017).
39. Franco-Salinas, G., de la Rosette, J. J. M. C. H. & Michel, M. C. Pharmacokinetics and pharmacodynamics of tamsulosin in its modified-release and oral controlled absorption system formulations. *Clin. Pharmacokinet.* **49**, 177–188 (2010).
40. Wang, X.-D. et al. Rapid and simultaneous determination of nifedipine and dehydronifedipine in human plasma by liquid chromatography-tandem mass spectrometry: Application to a clinical herb-drug interaction study. *J. Chromatogr. B* **852**, 534–544 (2007).
41. Vignoli, G. *Urodynamics: A Quick Pocket Guide* 175–184 (Springer, 2017).

Acknowledgements

We thank A. LaRochelle and K. Wood of CBSET, Inc. for providing discarded porcine ureters used for experimentation; F. McGovern, A. Feldman and D. Dahl of Massachusetts General Hospital Department of Urology for providing human ureteral tissue samples intraoperatively; C. Beale, L. Reyelt, C. Bogins and M. Hull of Tufts Surgical Research for providing discarded porcine ureters and assisting with in vivo surgical validation and protocol design; N. Enzer, K. Cormier and G. Ekchian of the Koch Institute for primary cell line, histopathological consultations and lubricant mixing equipment, respectively; C. Lewis of the Whitehead Institute Metabolomics Core for LCMS validation; L. Richey of Tufts Comparative Pathology Services for histopathological verification and consultation related to in vivo studies; D. Logan and M. Bray of the Broad Institute for CellProfiler assistance; N. Hawes (Nicola Hawes Design) for all figure schematics. We acknowledge funding support from M. Cima, the MIT Institute of Medical Engineering and Science Broshy Fellowship (C.X.L.) and the MIT Deshpande Center for Technological Innovation (C.X.L., M.J.C. and B.H.E.). This work was also supported in part by the Koch Institute Support (core) Grant P30-CA14051 from the National Cancer Institute and the National Institutes of Health (R35 GM122547 to A.E.C.).

Author contributions

C.X.L., M.J.C. and B.H.E. conceived the overall study and participated in manuscript writing. C.X.L. participated in and led all experimental work and manuscript writing. J.H.C. conducted automated screening experimentation and assay design, UV-absorbance quantification and assisted with manuscript writing. B.H.E. performed surgical in vivo validation, coordination of human tissue donors and assisted with manuscript writing. C.K.S. designed the screening automation. H.D. and C.A.W. assisted with all in vitro and in vivo data analysis. K.K. and A.E.C. assisted with CellProfiler data analysis and algorithm design. A.A.B. assisted with deriving hUSMC cultures from human donors. K.S.S. assisted with study design and manuscript editing.

Competing interests

The authors declare no competing interests.

Additional information

Supplementary information is available for this paper at https://doi.org/10.1038/s41551-019-0482-4.

Correspondence and requests for materials should be addressed to M.J.C.

nature research

Corresponding author(s): Michael J. Cima

Last updated by author(s): Oct 7, 2019

Reporting Summary

Nature Research wishes to improve the reproducibility of the work that we publish. This form provides structure for consistency and transparency in reporting. For further information on Nature Research policies, see Authors & Referees and the Editorial Policy Checklist.

Statistics

For all statistical analyses, confirm that the following items are present in the figure legend, table legend, main text, or Methods section.

n/a	Confirmed	
☐	☒	The exact sample size (*n*) for each experimental group/condition, given as a discrete number and unit of measurement
☐	☒	A statement on whether measurements were taken from distinct samples or whether the same sample was measured repeatedly
☐	☒	The statistical test(s) used AND whether they are one- or two-sided *Only common tests should be described solely by name; describe more complex techniques in the Methods section.*
☒	☐	A description of all covariates tested
☒	☐	A description of any assumptions or corrections, such as tests of normality and adjustment for multiple comparisons
☐	☒	A full description of the statistical parameters including central tendency (e.g. means) or other basic estimates (e.g. regression coefficient) AND variation (e.g. standard deviation) or associated estimates of uncertainty (e.g. confidence intervals)
☐	☒	For null hypothesis testing, the test statistic (e.g. *F*, *t*, *r*) with confidence intervals, effect sizes, degrees of freedom and *P* value noted *Give P values as exact values whenever suitable.*
☒	☐	For Bayesian analysis, information on the choice of priors and Markov chain Monte Carlo settings
☒	☐	For hierarchical and complex designs, identification of the appropriate level for tests and full reporting of outcomes
☒	☐	Estimates of effect sizes (e.g. Cohen's *d*, Pearson's *r*), indicating how they were calculated

Our web collection on statistics for biologists contains articles on many of the points above.

Software and code

Policy information about availability of computer code

Data collection	Computer-vision-aided cell segmentation and fluorescence-intensity values obtained via the open-source program CellProfiler. The custom analytical CellProfiler pipeline is provided as Supplementary Information.
Data analysis	Data analyses for drug hits and synergy were done with NumPy (a software package for scientific computing with Python). Analyses of ex vivo and in vivo pressure profiles were performed with MATLAB. Graph Pad Prism 7 was used for plotting the data.

For manuscripts utilizing custom algorithms or software that are central to the research but not yet described in published literature, software must be made available to editors/reviewers. We strongly encourage code deposition in a community repository (e.g. GitHub). See the Nature Research guidelines for submitting code & software for further information.

Data

Policy information about availability of data

All manuscripts must include a data availability statement. This statement should provide the following information, where applicable:

- Accession codes, unique identifiers, or web links for publicly available datasets
- A list of figures that have associated raw data
- A description of any restrictions on data availability

The data supporting the results in this study are available within the paper and its Supplementary Information. The raw datasets generated during the study are available from the corresponding author on request.

Field-specific reporting

Please select the one below that is the best fit for your research. If you are not sure, read the appropriate sections before making your selection.

☒ Life sciences ☐ Behavioural & social sciences ☐ Ecological, evolutionary & environmental sciences

For a reference copy of the document with all sections, see nature.com/documents/nr-reporting-summary-flat.pdf

Life sciences study design

All studies must disclose on these points even when the disclosure is negative.

Sample size	5 unique human, patient-derived, normal ureter smooth-muscle cell lines were developed and used for the experiments. A sample size of 3 is considered standard practice for the replication of high-throughput screening; 5 primary human cell lines is more than sufficient (https://doi.org/10.1038/nbt1186). Human-ureter specimens were collected over a period of 6 months. 10 porcine ureters were used ex vivo. Sample size was limited ultimately due to the quantity of suitable pigs for post-mortem harvest, since none were acquired solely for ureteral tissue. Samples collected over period of 18 months. In vivo studies were conducted in 3 pigs.
Data exclusions	No data was excluded from the in vitro screening. No data was excluded from the in vivo validation. Data from ureters that could not be stimulated to contract ex vivo were excluded. This exclusion criteria was pre-established, as it was deemed that these ureters were no longer viable and that sample viability was lost during transportation.
Replication	Initial screening runs were performed across 3 patient cell lines in biological replicates, with the data averaged. After selection of drug candidates, all experiments were screened across 5 patient cell lines in biological replicates with the data averaged. For each of the five ex vivo conditions, 2 discarded ureters were tested as biological replicates. Data was combined and averaged for each condition. For each of the three in vivo pigs, all pigs received the same sets of interventions, with the data combined and averaged.
Randomization	The 3 pigs tested in vivo were randomly assigned to receive either oral tamsulosin or topical therapy first. No other randomization was needed for other aspects of the study.
Blinding	Not applicable.

Reporting for specific materials, systems and methods

We require information from authors about some types of materials, experimental systems and methods used in many studies. Here, indicate whether each material, system or method listed is relevant to your study. If you are not sure if a list item applies to your research, read the appropriate section before selecting a response.

Materials & experimental systems

n/a	Involved in the study
☐	☒ Antibodies
☐	☒ Eukaryotic cell lines
☒	☐ Palaeontology
☐	☒ Animals and other organisms
☐	☒ Human research participants
☒	☐ Clinical data

Methods

n/a	Involved in the study
☒	☐ ChIP-seq
☒	☐ Flow cytometry
☒	☐ MRI-based neuroimaging

Antibodies

Antibodies used	Phospho-Myosin Light Chain 2 (Thr18/Ser19) Antibody, Cell Signaling Technology (Catalog #3674); Goat anti-Rabbit IgG (H+L) Cross-Adsorbed Secondary Antibody, Alexa Fluor 488, ThermoFisher Scientific (Catalog #A-11008). Multiple lots used for all antibodies.
Validation	Validation of phospho-myosin light chain antibody: https://www.cellsignal.com/products/primary-antibodies/phospho-myosin-light-chain-2-thr18-ser19-antibody/3674?site-search-type=Products&N=4294956287&Ntt=diphospho+myosin+light+chain&fromPage=plp Validation of AlexaFluor 488 antibody: https://www.thermofisher.com/antibody/product/Goat-anti-Rabbit-IgG-H-L-Secondary-Antibody-Polyclonal/A-11008

Eukaryotic cell lines

Policy information about cell lines

Cell line source(s)	Patient-derived primary normal ureteral smooth muscle cells (not commercially available).
Authentication	None of the primary cell lines used were authenticated by STR analysis. There are no commercially available reference cell lines for authentication comparison.
Mycoplasma contamination	Cell lines were tested for mycoplasma initially after derivation from whole tissue, and monthly when in culture. The Lonza MycoAlert kit was used. All 5 primary cell lines tested negative for mycoplasma at all times.
Commonly misidentified lines (See ICLAC register)	Not applicable.

Animals and other organisms

Policy information about studies involving animals; ARRIVE guidelines recommended for reporting animal research

Laboratory animals	Adult (70kg) female domestic swine (Sus scrofa) were obtained from Tufts Cummings Veterinary Medical Center (North Grafton, MA).
Wild animals	The study did not involve wild animals.
Field-collected samples	The study did not involve samples collected from the field.
Ethics oversight	The use of all biological samples and animal specimens were approved by corresponding institutional IRB and IACUC protocols. The use of human-derived primary ureteral smooth muscle cells was approved by the Massachusetts Institute of Technology Committee on the Use of Humans as Experimental Subjects (COUHES), and covered by MIT COUHES protocol #1508154982. Ex vivo porcine ureter specimens were obtained via MIT IACUC-approved discarded-tissue-exchange protocols, covered by MIT protocol CIMA-E14-08-0617. All animal work is covered under MIT Protocol CIMA-117-107-OS and Tufts Medical Center Protocol B2017-114. All in vivo animal experimentation was approved by the MIT and Tufts IACUC IRBs.

Note that full information on the approval of the study protocol must also be provided in the manuscript.

Human research participants

Policy information about studies involving human research participants

Population characteristics	Patients undergoing radical cystectomy or nephrectomy were selected as candidates for providing discarded ureter tissue. Patient selection included otherwise health patients with localized urological disease without prior history of infectious or contagious diseases. Negative tumor margins on the ureter were confirmed intraoperatively.
Recruitment	No recruitment was performed. Human participation for this study fell under 'discarded tissue transfer', which is a common method of sourcing human-derived tissue. Patient consent was not required for transfering discarded and de-identified tissue samples.
Ethics oversight	No direct patient contact was required, and no patient identifiers were needed. No patient consent was required because the ureters were considered 'discarded', and no patient identifiers were recorded in connection with the tissue samples. Primary IRB is held at Massachusetts General Hospital (Boston, MA). MIT Protocol COUHES IRB #1508154082.

Note that full information on the approval of the study protocol must also be provided in the manuscript.